Biochemical and Biophysical Research Communications 387 (2009) 164–168

Contents lists available at ScienceDirect

Biochemical and Biophysical Research Communications

journal homepage: www.elsevier.com/locate/ybbrc

Functionalized silicon quantum dots tailored for targeted siRNA delivery

S. Klein [a], O. Zolk [b], M.F. Fromm [b], F. Schrödl [c,d], W. Neuhuber [c], C. Kryschi [a,*]

[a] Department Chemistry and Pharmacy, Physical Chemistry I and ICMM, Friedrich-Alexander University of Erlangen-Nuremberg, Egerlandstr. 3, D-91058 Erlangen, Germany
[b] Institute of Experimental and Clinical Pharmacology and Toxicology, Friedrich-Alexander University of Erlangen-Nuremberg, Fahrstr. 17, D-91054 Erlangen, Germany
[c] Institute of Anatomy I, Friedrich-Alexander University of Erlangen-Nuremberg, Krankenhausstr. 9, D-91054 Erlangen, Germany
[d] Departments of Anatomy/Ophthalmology, Paracelsus Medical University, Strubergasse 21, A-5020 Salzburg, Austria

ARTICLE INFO

Article history:
Received 19 June 2009
Available online 2 July 2009

Keywords:
Silicon quantum dots
siRNA delivery
MDR1
P-glycoprotein
Caco-2 cells

ABSTRACT

For RNA interference (RNAi) mediated silencing of the *ABCB1* gene in Caco-2 cells biocompatible luminescent silicon quantum dots (SiQDs) were developed to serve as self-tracking transfection tool for *ABCB1* siRNA. While the 2–3 nm sized SiQD core exhibits green luminescence, the QD surfaces are completely saturated with covalently linked 2-vinylpyridine that may electrostatically bind siRNA. For down-regulating P-glycoprotein (Pgp) expression of the *ABCB1* gene the SiQDs were complexed with siRNA. The cellular uptake and allocation of SiQD–siRNA complexes in Caco-2 cells were monitored using confocal laser scanning microscopy and transmission electron microscopy. The release of siRNA to the cytoplasm was verified through real-time PCR quantification of the reduced *ABCB1* mRNA level. Additional evidence was obtained from time-resolved in situ fluorescence spectroscopic monitoring of the Pgp efflux dynamics in transfected Caco-2 cells which yielded significantly reduced transporter efficiencies for the Pgp substrate Rhodamine 123.

Introduction

RNA interference (RNAi) is a post-transcriptional gene silencing mechanism for regulating gene expression during development [1–3]. RNAi was first observed in the nematode worm *Caenorhabditis elegans*, where the incorporation of long double-stranded RNA led to targeted degradation of homologous mRNA [4]. Prospect of utilizing this gene silencing mechanism for biomedical research and therapy has been raised, when Tuschl et al. [5] verified that RNAi in mammalian cells may be mediated by 21- and 22-nucleotide RNAs serving as effector molecules of sequence-specific gene silencing. Therefore the antisense (guide) strand of the short interfering, double-stranded RNA (siRNA) is incorporated into a RNA-induced silencing complex (RISC). Gene silencing is achieved when the antisense strands of the siRNA guide the RISCs to homologous mRNA in the cell. The RNA endonucleases in the RISCs provide sequence-specific cleavage of mRNAs and thereupon down-regulating of protein expression. Therapeutic applications of siRNAs require their in vivo delivery into the target cell. This remains a major hurdle for RNAi therapy, since naked siRNA may not cross the mammalian cell membrane. In addition, many of the transfection methods used for in vitro studies cannot be used in most in vivo settings.

One promising strategy for in vivo delivering siRNAs into cells is based on luminescent semiconductor quantum dots (QDs) as allowing for tracking the transfection and allocation of QD–siRNA complexes in the cytoplasm [6–9]. For instance, luminescent CdSe/ZnS QDs was co-delivered along with siRNA using the cationic liposome Lipofectamine 2000 [6]. Down-regulation of the lamin a/c gene in murine fibroplasts could be directly correlated with intracellular fluorescence. Since Liptofectamine itself acts as carrier for siRNA, it remains unclear to which extent the QDs will be conducive to siRNA delivery. Moreover, uncoated CdSe/ZnS QDs are toxic to cells because of their release of Cd^{2+} ions into the cytoplasm and subsequent binding to sulfohydryl groups of mitochondria proteins resulting in decreased mitochondrial respiration [10]. The cytotoxicity of CdSe/ZnS QDs could be successfully reduced by coating with polymers, polyethyleneglycol (PEG), chitosan or silica [7–9]. Using CdSe/ZnS QDs as luminescent core Derfus et al. developed a multifunctional nanoparticle platform that serves as targeted and self-tracking vehicles for siRNA delivery [9]. Therefore, the QD surfaces were functionalized with siRNA via chemical cross-linkers and targeting cell-surface F3 peptides. Although the F3 peptide provided targeted cellular internalization, no gene silencing was observed. One reason for this might be the very bulky peptide structure hampering the F3/siRNA–QD complex to escape the endosome. Another approach for self-tracked delivery of siRNA was accomplished by Tan et al. [8] upon synthesizing 60 nm-sized chitosan nanoparticles with encapsulated

* Corresponding author. Address: Department of Physical Chemistry I, Friedrich-Alexander University, Egerlandstr. 3, D-91058 Erlangen, Germany. Fax: +49 9131 8528967.
E-mail address: kryschi@chemie.uni-erlangen.de (C. Kryschi).

0006-291X/$ - see front matter © 2009 Elsevier Inc. All rights reserved.
doi:10.1016/j.bbrc.2009.06.144

CdSe/ZnS Qds. The adverse feature of these conjugates is the rather slow release dynamics of the siRNA in the cytoplasm which started to take place after 2 days.

In the present study, luminescent SiQD functionalized with 2-vinylpyridine were developed to serve as self-tracking vehicle for siRNA delivery in tumor cells. Our research objective was to temporarily down-regulate via RNAi the P-glycoprotein (Pgp) expression of the multidrug resistant gene 1 (*MDR1*, symbol approved by the HUGO Gene Nomenclature: *ABCB1*) in a human colon carcinoma cell line (Caco-2) as representing an in vitro cell model for the enterocytes of the gastro-intestinal tract [11,12]. Pgp often invalidates cancer chemotherapy because of its overproduction in tumor cells giving rise to multidrug resistance [13]. SiQDs dispersed in aqueous solutions were shown to form complexes with *ABCB1* siRNA and to act as vehicle for siRNA delivery into Caco-2 cells. The release of siRNA in the cytosol with subsequently RNAi induced down-regulation of the Pgp translation was substantiated to take place by determining a reduced *ABCB1* mRNA level in transfected Caco-2 cells using real-time PCR. Additional evidence for successful *ABCB1* gene silencing was obtained by measuring a significant decrease of the Pgp transporter efficiency for the fluorescent substrate Rhodamine 123 (Rh123). Both, transcellular transport study and real-time PCR analysis were performed with SiQD–siRNA complexes and Lipofectamine 2000 as reference transfection tool for *ABCB1* siRNA.

Materials and methods

Chemicals. Rhodamine 123 (Rh123), 2-ethynylpyridine (Aldrich, 98%), *o*-xylene anhydrous (Aldrich, 97%), ethanol (Merck), aqueous hydrofluoric acid (Riedel-de Haën, 40%) were used as received. Lipofectamine 2000, DMEM, L-glutamine, FBS, penicillin–streptomycin-solution, sodium pyruvate solution, PBS, MEM, Optimem and trypsin/EDTA were purchased from Invitrogen. Sodium dodecylsulfate (90%), MTT (98%), HEPES sodium salt (99%) and D-(+)-glucose were obtained from Aldrich and glutardialdehyde (25%) from Roth. Sodium chloride (99.5%) and potassium chloride (99.5%) was from Fluka and sodium hydrogen carbonate (99.5%) from Merck. In situ Cell Death Detection Kit, TMR red was supplied by Roche Applied Science. The processed SiQDs had a mean size of 5 nm and were fabricated by Evonik Degussa–Creavis Technologies & Innovation in a low-pressure microwave reactor using silane as a precursor.

Cell culture. Caco-2 cells were cultured in DMEM containing 4.5 g/l D-glucose (Invitrogen, Karlsruhe, Germany) which was enriched with 10% fetal bovine serum (FBS), 1 mM sodium pyruvate, 100 U/ml penicillin, 100 μg/ml streptomycin, 2 mM GlutaMAX™-I supplement, 1% MEM nonessential amino acids (Invitrogen, Karlsruhe, Germany). Cells were incubated at 37 °C in a 10% CO_2/air incubator with 90% humidity. Cells were sub-cultivated twice a week.

Functionalization of SiQDs. H terminated SiQDs were obtained by HF etching the oxidized QD surface using a 10% HF/ethanol solution. Subsequently a thermal hydrosilylation procedure using as reagent 2-ethynylpyridine in m-xylene were carried out and oxide-free, water-soluble, green luminescent 2-vinylpyridine terminated SiQDs with sizes between 2 and 3 nm were obtained [15].

SiQD–siRNA and Lipofectamine–siRNA complexes. For down-regulating the Pgp expression of the *ABCB1* gene in Caco-2 cells 1 nmol of the mixture *ABCB1* siRNA sense (UUCAAGAUCCAGUCUAAU AAGAAA[dT][dT]) and *ABCB1* siRNA antisense (UUUCUUAUUAGAC UGGAUCUUGAA[dT][dT]) were purchased (SigmaOligos, Aldrich). 1 mg 2-vinylpyridine terminated SiQDs were dispersed in 1 ml nuclease-free water. 50 μl of this stock solution was mixed gently with 45 pmol *ABCB1* siRNA duplexes diluted in 50 μl Optimem (OptiMEM, Gibco) for each well and incubated for 20 min at room temperature to allow the complexes to form. Reference knockdown experiments were executed using Lipofectamine 2000 as transfection tool for *ABCB1* siRNA.

Agarose gel electrophoresis. SiQD–siRNA complexes were prepared by mixing in nuclease-free water and electrophoresed on 1% agarose gel for 60 min at 100 V. siRNA was visualized by ethidium bromide staining. Electrophoresis images of free siRNA and SiQD–siRNA complexes were taken using the GelDoc 2000 imager system (Bio-Rad, Munich, Germany).

Confocal laser scanning microscopy. Caco-2-cells were seeded on *Lab-Tek*™ Chamber Slide™, one well (Nunc, Germany) and incubated with SiQD (75 μg/ml) for 24 h. Two dimensional confocal fluorescence microscopy was used for documentation of cellular uptake of SiQDs (Bio-Rad MRC 1000 microscope attached to a Nikon Diaphot 300 and equipped with a krypton–argon laser; 20 × dry or 40 × and 60 × oil-immersion objective lenses, with numeric apertures of 0.75, 1.30, and 1.4, respectively). Images were created in the single optical section mode using 488 nm excitation and the appropriate filter (605DF32; Nikon).

Transmission electron microscopy (TEM). Caco-2 cells incubated with SiQDs solutions were washed in PBS, fixed in phosphate-buffer containing 2.5% glutaraldehyde (4 h at 4 °C) and subsequently postfixed with a solution containing 1% osmium tetroxide and 3% potassium ferricyanide at room temperature. Cells were dehydrated through graded alcohols, embedded in Epon and mounted on Epon blocks. Semithin sections were stained with methylene blue, and silver–grey ultrathin sections were contrasted with uranyl acetate and examined in a Zeiss 906 transmission electron microscope (LEO, Oberkochen, Germany).

Real-time PCR analysis. Total RNA was extracted from Caco-2 cells with Trizol reagent (Invitrogen, Carlsbad, CA, USA). Total RNA (2 μg each) was reverse-transcribed, and complementary deoxyribonucleic acid (cDNA) was subsequently amplified with the LightCycler system (Roche Applied Science, Mannheim, Germany). Primers for *ABCB1* (forward: 5′-tggagagatcctcaccaagc-3′; reverse: 5′-ttcctgtcccaagatttgct-3′) and *ACTB* (forward: 5′-tgacgg ggtcacccacactgtgcccatcta-3′; reverse: 5′-ctagaagcatttgcggtggacga tggaggg-3′) were designed to amplify fragments crossing exon/exon boundaries. For each amplified DNA product, a melting curve analysis was carried out. Polymerase chain reaction (PCR) products were further analyzed by agarose gel electrophoresis and sequencing to confirm the identity of the PCR products and to exclude the possibility of chromosomal DNA artifacts. The level of *ACTB* (β-actin) mRNA in each sample was used for normalization.

Cytotoxicity of the SiQDs was assessed by MTT (3-(4,5-dimethyldiazol-2-yl)-2,5-diphenyltetrazolium bromide) cell viability assay and TUNEL assay. For the MTT assay Caco-2 cells were incubated with SiQD (10 μg/ml) in medium and serum- and aminoacid-free HEPES buffer (B2 buffer), which is necessary for the transport studies. B2 buffer was prepared by us containing sodium chloride (154 mM), potassium chloride (5.6 mM), HEPES (20 mM), D-glucose (5 mM) and sodium hydrogen carbonate (25 mM). After 1, 2, 4 and 24 h the cells were washed with phosphate-buffer and incubated for 1 h with 0.5 mg/ml MTT dissolved in PBS solution. The cell viability was determined by measuring the absorbance of the purple MTT metabolite formazan solution at 590 nm. For TUNEL assay, a commercially available in situ cell death detection kit (Roche Applied Science) was used for labeling the ends of DNA fragments. Caco-2 cells either exposed to SiQDs (75 μg/ml for 48 h) or treated with Dnase I recombinant were fixed with PBS containing 4% paraformaldehyde, and further processed following manufacture's protocol. The apoptotic cells were visualized using standard fluorescence microscopy (Aristoplan, Leica, Germany equipped with a RT color digital camera, Diagnostic Instruments, Sterling Heights, USA).

Intracellular transport study. Caco-2 cells were grown as epithelial layers by seeding them at a density of 2×10^5 cells/well on polycarbonate Transwell™ filters (Corning, Schiphol-Rijk, The Netherlands) and studies were performed 14 days after plating. Afterwards cells were transfected with SiQD–siRNA or Lipofectamine–siRNA. To ensure cell monolayer integrity the transepithelial electrical resistance (TEER) was measured before and after each experiment using the Millicell–ERS system (Millipore, Schwalbach, Germany). Rhodamine 123 (Rh123) dissolved at 0.1 mM in serum and aminoacid-free B2 buffer. This buffer was used because of the fluorescent substances in DMEM and Optimem and its high cell viability. The Rh123 solution was added to the donor compartment and the Rh123 transport in secretory direction was monitored by measuring the fluorescence intensity in the acceptor compartment as function of time using a home-made in situ fluorescence detector device [14]. The functional changes in the efflux due to *ABCB1* knockdown was measured over a period of 10 days performing a transport study each day for 5 h.

Statistical analysis. Data are presented as arithmetic means ± SE. Statistical analysis was performed using Student's *t*-test to compare two groups and analysis of variance (ANOVA) with post hoc Bonferroni correction for multiple comparisons. A value of $p < 0.05$ was considered statistically significant. Two-way ANOVA was used for statistical analysis of transport curves.

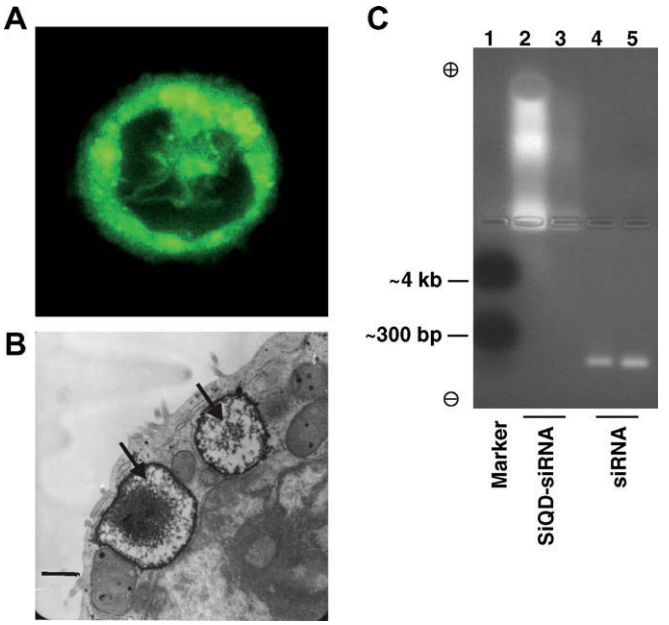

Fig. 1. Cellular uptake of SiQDs as shown by CLSM (A) and TEM (B) imaging: the CLSM image shows the green emission from internalized SiQD; the arrows in the TEM image indicates to endosomes containing the SiQDs (scale bar = 750 nm); The formation of SiQD–siRNA complexes visualized by agarose gel electrophoresis (C): the bright bands in lanes 1 and 2 extending from the slots to the cathode (⊕) arise from SiQDs–siRNA complexes (electrically neutral) and free (positively charged) SiQDs. The distinct bands in lanes 3 and 4 indicate free siRNA migrating to the anode (⊖).

Results and discussion

Due to quantum confinement 2-vinylpyridine terminated SiQDs with sizes between 2 and 3 nm exhibit green photoluminescence with quantum yields around 30% [15]. Moreover these SiQDs are soluble in water and the pyridine ligands, acting as Brönstedt base, provide positive charges at the SiQD surfaces.

To evaluate the potential application of these functionalized SiQDs for gene delivery, in vitro transfection experiments were conducted on Caco-2 cells targeting the *ABCB1* gene. The essential steps in the use of SiQDs for siRNA are (1) the formation of SiQD–siRNA complexes, (2) the cellular internalization of the SiQD–siRNA and (3) the subsequent release of the siRNA to cell cytoplasm followed from incorporation in the RISC.

The internalization of SiQDs by Caco-2 cells was studied using transmission electron microscopy (TEM) and confocal laser scanning microscopy (CLSM). For CLSM imaging the SiQD luminescence was excited at 488 nm and detected between 510 and 530 nm. The luminescence micrograph clearly visualizes the cellular uptake of the green luminescent SiQDs and their accumulation outside the cell nucleus (Fig. 1A). Using TEM, we could provide more detailed information regarding the location and internalization mechanisms of the SiQDs: since they accumulate in endosomes (see black arrows in Fig. 1B), endocytosis is the most obvious mechanism.

Incubation of SiQDs with *ABCB1* siRNA in nuclease-free water for 10 min resulted into the formation of SiQD–siRNA, as shown by agarose gel electrophoresis (Fig. 1C). While unbound, negatively charged siRNA (Fig. 1C: fourth and fifth lane) and free, positively charged SiQDs (Fig. 1C: second and third lane) migrated towards the anode and cathode, respectively, the bright bands remaining at the slots (Fig. 1C, second and third lane) indicate electrically neutral SiQD–siRNA complexes.

The release of *ABCB1* siRNA from the endosome into the cytosol is expected to result into activation of the RISC complex and specific cleavage of the *ABCB1* mRNA. Therefore, siRNA that reached the cytosol and started the RNAi machinery can be tracked by monitoring gene silencing, *i.e.* by detecting the decline in mRNA levels of the specific target gene in transfected cells. We investigated the efficacy of gene silencing by use of SiQD in comparison with a liposomal carrier for siRNA. Lipofectamine 2000 was chosen for comparison, since this liposomal transfection reagent is commercially available and widely used and thus served as a reference in some previous studies. Real-time PCR was used to analyze the *ABCB1* mRNA level in untreated and transfected Caco-2 cells, in which the transfection was carried out by incubating the cells with SiQD–siRNA or Lipofectamine–siRNA complexes, respectively (Fig. 2). While the delivery of *ABCB1* siRNA accomplished with Lipofectamine 2000 led to a reduction of the mRNA level in untreated Caco-2 cells (Fig. 2: grey bar) by 71%, siRNA transfection through SiQDs decreased the mRNA by 50%. This result demonstrates for SiQD–siRNA significant transfection efficiency.

Reduction of the *ABCB1* mRNA level in Caco-2 cells by RNAi leads to silencing of the *ABCB1* gene and thereupon to transient down-regulation of the Pgp translation. Since Pgp acts as trans-

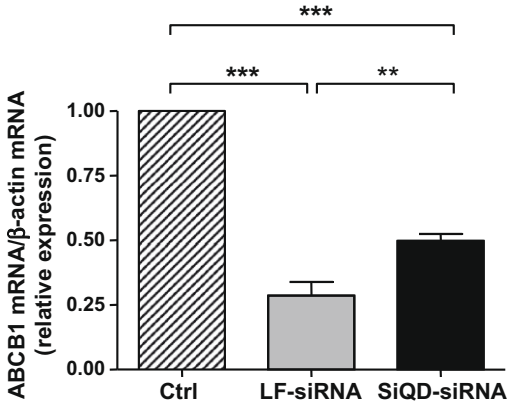

Fig. 2. Real-time PCR analysis of the *ABCB1* mRNA level of Caco-2 cells that were non-transfected (white bar), transfected with siRNA using Lipofectamine 2000 as carrier (grey bar) and transfected through siRNA delivery by SiQD vehicle (black bar), $n = 4$; $^{**}p < 0.01$; $^{***}p < 0.001$.

porter protein for a wide spectrum of compounds, successful silencing of the *ABCB1* gene can be verified by detecting reduced efflux efficiency of Pgp. To this end, transcellular transport studies were performed, and Pgp mediated transport of the fluorescent substrate Rh123 across Caco-2 cell monolayers were measured using an in situ fluorescence spectroscopy technique. Therefore the Caco-2 cells were transfected with *ABCB1* siRNA using SiQDs or Lipofectamine 2000 as delivery cargo. The Caco-2 cells were cultured as a confluent monolayer on a permeable polycarbonate, in order to stimulate the polarization of the Caco-2 cells and therewith the Pgp expression on their apical surfaces. The Pgp transporter activity was evaluated by measuring the secretory (basolateral-to-apical) efflux of Rh123 in Caco-2 cells. The time profiles of the transcellular transport across the cell monolayer were obtained for Caco-2 cells transfected by Lipofectamine–siRNA or SiQD–siRNA complexes (Fig. 3, top). Both transfection tools led to a similar temporal behavior of the uptake curves: from day 0 to day 8 post-transfection the secretory transport of Rh123 continuously dropped off ($p < 0.05$, two-way ANOVA) for Lipofectamine 2000 and SiQDs, respectively. This marked decrease of secretory flux of Rh123 indicates RNAi induced down-regulation of the expression of Pgp at the apical sides of the Caco-2 cells which correlates with the observed decrease in *ABCB1* mRNA levels, as determined by real-time PCR analysis.

We also addressed the question of cytotoxic side effects of SiQDs. A number of methods have been developed to study factor-mediated cytotoxicity. We used the TUNEL assay as a measure of apoptosis as well as the colorimetric MTT assay as a measure of metabolic activity and cell proliferation. Because the tetrazolium salt MTT is reduced to a purple formazan dye only by metabolically active cells, this assay detects viable cells exclusively. Fig. 3 (bottom) depicts the absorbance of the MTT metabolite formazan in Caco-2 cells exposed to SiQD for 1, 2, 4 and 24 h relative to control cells without SiQDs. Regardless of whether medium (with all supplements including serum) or a serum- and aminoacid-free B2 buffer was used, SiQDs had no short-term effects on the metabolic activity of the cells. 24 h after start of the SiQD incubation a slight decrease in the absorption of formazan was detected only in cells incubated in B2 buffer. To investigate the specific impact of SiQDs on apoptosis in Caco-2 cells, TUNEL assays were performed. TUNEL-positive cells were distinguished as cells with condensed, fragmented and intensely stained nuclei. The results of the TUNEL assay for Caco-2 cells with internalized SiQDs, Caco-2 cells treated with a specific DNA cleavage enzyme and untreated cells (reference cells) are visualized by fluorescence micrographs of the fluorescent apoptic reference cells and dark Caco-2 cells with SiQDs (Fig. 4). This result is consistent with that obtained from MTT assay and confirms absence of major cellular toxicity of the SiQDs in vitro.

Conclusions

In this study, we present a novel class of transfection tools that are based on biocompatible, water-soluble luminescent SiQDs. The internalization of the SiQDs by Caco-2 cells as observed by TEM and CLSM imaging studies occurs via endocytosis. Experiments employing agarose gel electrophoresis revealed positive charging of the SiQDs in aqueous solutions and the SiQD–siRNA complexes are formed through electrostatic interactions. As indirectly shown by real-time PCR and transcellular transport studies, the functionalized SiQDs achieve high gene-transfection efficiency for *ABCB1* siRNA which they delivered to the cytosol of Caco-2 cells. Release and incorporation of siRNA into the RISC were tracked by detecting the reduced *ABCB1* mRNA level and the decreased Pgp transporter efficiency of successfully transfected Caco-2 cells. SiQDs pose only

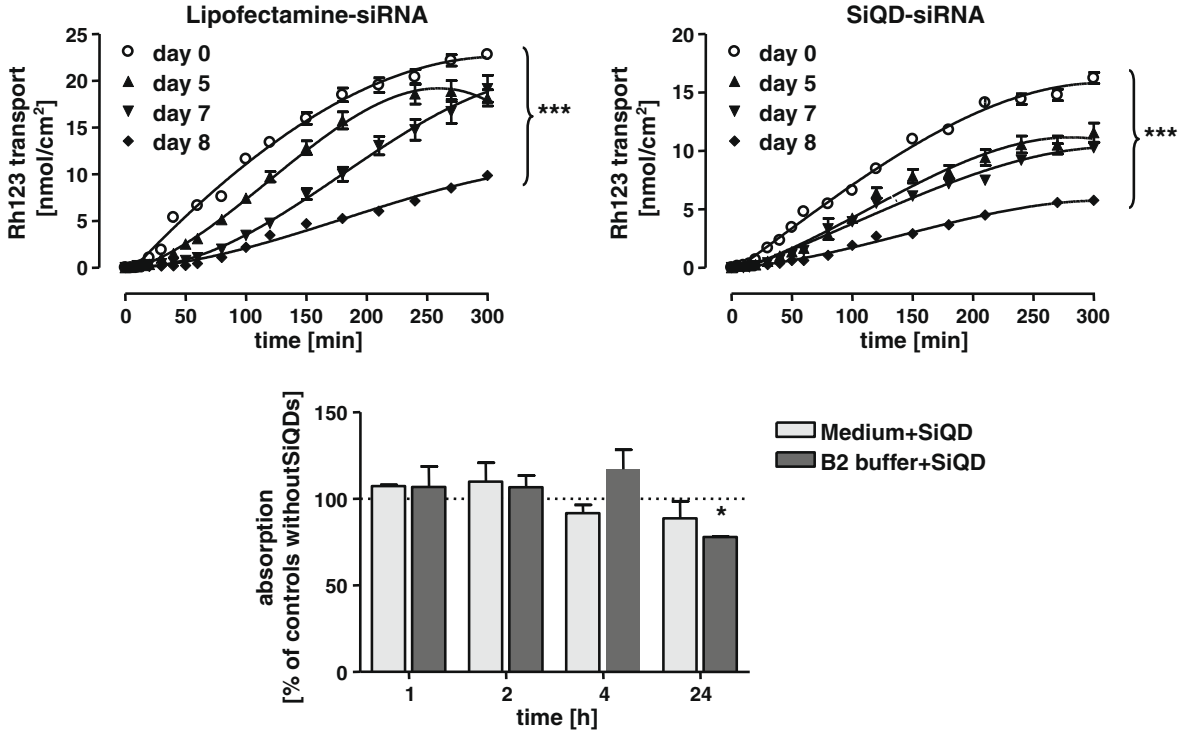

Fig. 3. Transcellular transport studies of the Pgp mediated secretory efflux of Rh123 across the monolayer of Caco-2 cells transfected by Lipofectamine–siRNA (top, left) and SiQD–siRNA complexes (top, right) at 37 °C; the time profiles of the relative transport rate [%] after different periods (days) subsequently to the cell transfection. $n = 3$; $^{***}p < 0.0001$ for the effect of the time post-transfection on the transport curves (two-way ANOVA); MTT assay of Caco-2 cells incubated in medium and B2 buffer with and without SiQDs (bottom); $^{*}p > 0.05$.

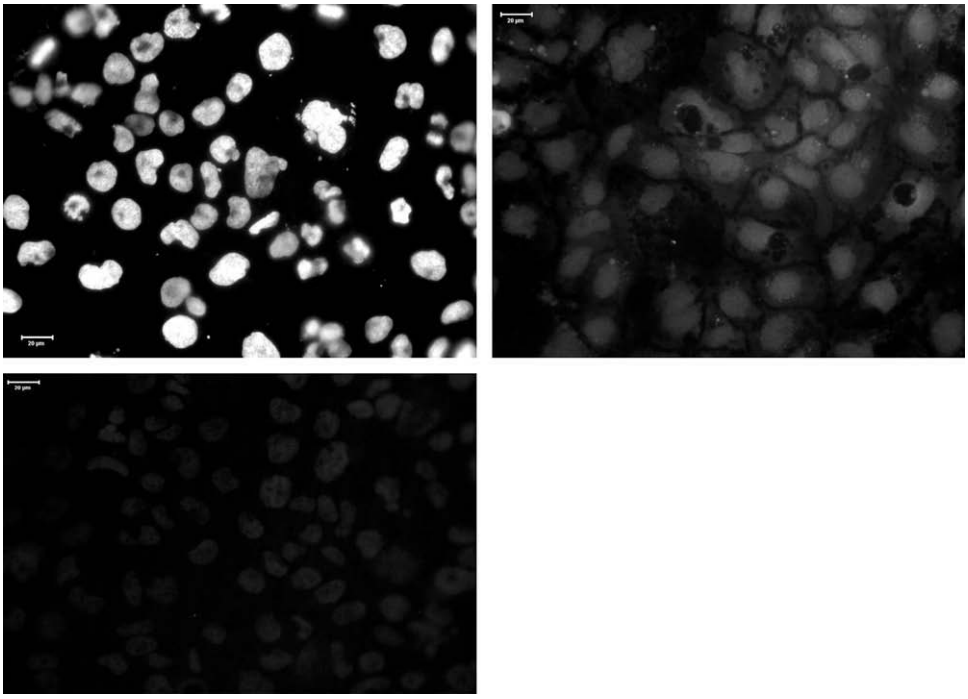

Fig. 4. TUNEL assay of untreated Caco-2 cells (top, left), cells incubated in the presence of SiQDs (top, right) or treated with a specific DNA cleavage enzyme (bottom).

negligible effect on both viability and apoptosis of Caco-2 cells as demonstrated by MTT and TUNEL assays.

Acknowledgments

Support of the Deutsche Forschungsgemeinschaft (Graduiertenkollegs 1161/1) is gratefully acknowledged. We are grateful to Dr. André Ebbers (Evonik-Degussa-Creavis Technologies & Innovation) for generously providing us with Si qdots. We thank A. Hilpert and I. Zimmermann for TEM imaging studies as well as H. Symowski for technical assistance (all Institute of Anatomy I, University Erlangen-Nuremberg).

References

[1] D.H. Kim, J.J. Rossi, Strategies for silencing human diseases using RNA interference, Nat. Rev. Gen. 8 (2007) 173–184.
[2] D.M. Dykxhoorn, C.D. Novina, P.A. Sharp, Killing the messenger: short RNAs that silence gene expression, Nat. Rev. Mol. Cell Biol. 4 (2003) 457–467.
[3] D.M. Dykxhoorn, J. Lieberman, The silent revolution: RNA interference as basic biology, research tool and therapeutic, Annu. Rev. Med. 56 (2005) 401–423.
[4] A. Fire, S. Xu, M.K. Montgomery, S.A. Kostas, S.E. Driver, C.C. Mello, Potent and specific genetic interference by double-stranded RNA in *Caenorhabditis elegans*, Nature 391 (1998) 806–811.
[5] S.M. Elbashir, W. Lendeckel, T. Tuschl, RNA interference is mediated by 21–22 nucleotide RNAs, Genes Dev. 15 (2001) 188–200.
[6] A.A. Chen, A.M. Derfus, S.R. Khetani, S.N. Batia, Quantum dots to monitor RNAi delivery and improve gene silencing, Nucleic Acids Res. 33 (2005) e190.
[7] T. Zhang, J.L. Stilwell, D. Gerion, L. Ding, O. Elboudwarej, P.A. Cooke, J.W. Gray, A.P. Alivisatos, F.F. Chen, Cellular effect of high doses of silica-coated quantum dot profiled with high throughput gene expression analysis and high content cellomics measurements, Nano Lett. 6 (2006) 800–808.
[8] Wee Beng Tan, Shan Jiang, Yong Zhang, Quantum-dot based nanoparticles for targeted silencing of HER2/neu gene via RNA interference, Biomaterials 28 (2007) 1565–1571.
[9] A.M. Derfus, A.A. Chen, D.-H. Min, E. Ruoslahti, S.N. Bhatia, Targeted quantum dot conjugates for siRNA delivery, Bioconj. Chem. 18 (2007) 1391–1396.
[10] L.E. Rikans, T. Yamano, Mechanism of cadmium-mediated acute hepatotoxicity, J. Biochem. Mol. Toxicol. 14 (2000) 110–117.
[11] C. Pauli-Magnus, O. von Richter, O. Burk, A. Ziegler, T. Mettang, M. Eichelbaum, M.F. Fromm, Characterization of the major metabolites of verapamil as substrates and inhibitors of P-glycoprotein, J. Pharmacol. Exp. Ther. 293 (2000) 376–382.
[12] C. Loetchutinat, C. Saengkhae, C. Marbeuf-Gueye, A. Garnier-Suillerot, Eur. J. Biochem. 270 (2003) 476–485.
[13] U.A. Germann, Eur. J. Cancer 32A (1996) 927–944.
[14] C. Kryschi, A. Netter, Fluorescence spectroscopic in situ detection of pharmacokinetics of transporter proteins, German patent DE 10 2007 049 644 A1.
[15] C. Cimpean, V. Groenewegen, V. Kuntermann, A. Sommer, C. Kryschi, Ultrafast exciton relaxation dynamics in silicon quantum dots, Laser Photon Rev. 3 (2009) 138–146.